In a comparison of the catalytic activities of various metal oxides, the bonding of the allyl radical in terms of a π-complex with the metal cation appears to be a property common to all the catalysts which are active in oxidative dehydrogenation (*9*). Thus we may conclude that the existence of the allyl radical is an essential feature in the oxidation of propylene. However, the extent of oxidation or the selectivity of the catalyst is more likely controlled by the different species of oxygen present on the surface and in the lattice. This aspect of the problem has received attention in recent papers by other investigators (*10, 11*). The crude model for relating oxidation specificity to the metal–oxygen bond strength in the lattice has been refined by us in terms of different sorbed oxygen species, charged and neutral. It is the distribution of the various oxygen species that governs the specificity of the catalytic reaction (*1*).

REFERENCES

1. Wood, B. J., Wise, H., and Yolles, R., *J. Catal.* **15**, 355 (1969).
2. Schenck, R., and Kurzen, F., *Z. Anorg. Allg. Chem.* **235**, 97 (1937).
3. Schulz, I. W., Ebert, T., and Scheve, J., *Z. Anorg. Allg. Chem.* **346**, 66 (1966).
4. Keeley, W. M., and Mathes, W. B., *J. Chem. Eng. Data* **11**, 582 (1966).
5. Schenck, R., and Kurzen, F., *Z. Anorg. Allg. Chem.* **220**, 97–106 (1934).
6. Rienacker, G., *Z. Anorg. Allg. Chem.* **258**, 280 (1949).
7. Scheve, J., and Schulz, I. W., *Int. Congr. Catal., 4th, Moscow, 1968,* Prepr. 84.
8. Isaev, O. V., Margolis, L. Y., and Sazanova, I. S., *Dokl. Akad. Nauk SSSR* **129**, 141 (1959).
9. Adams, C. R., *Proc. Int. Congr. Catal., 3rd, 1964* **1**, 240 (1965).
10. Sachtler, W. M. H., and DeBoer, N. A., *Proc. Int. Congr. Catal., 3rd, 1964* **1**, 252 (1965).
11. Boreskov, G. K., *Discuss. Faraday Soc.* **41**, 263 (1966).

S. Henry Inami
Henry Wise

Solid State Catalyst Laboratory,
Stanford Research Institute,
Menlo Park, California 94025
Received December 10, 1969

Mass Transfer Effects in the Olefin Disproportionation Reaction

Preliminary propylene disproportionation studies on a WO_3–silica catalyst have shown increased catalyst efficiency with increased flow rate. This clearly indicates a mass transfer or interphase diffusional effect, although calculations made on the basis of generalized equations for diffusion predict no limitation in reaction rates by mass transfer (*1*). Such calculations use the external, catalyst surface area to estimate the area over which diffusion occurs. However, with few exceptions, only a very limited fraction of the total catalyst surface is active, and there is reason to question any *a priori* calculation which rules out interphase diffusion limitations on the basis of external surface area.

Runs were made using a split bed quartz reactor in which the propylene flow could be reversed. Gas samples were withdrawn after full or ½-bed contact with the catalyst. This split bed, reversible flow reactor allowed two catalyst specimens to be compared simultaneously under identical reaction conditions. Hence, direct comparisons were made between two different weights of catalyst as well as between two different particle sizes.

The disproportionation of propylene on cobalt molybdate–alumina catalyst at 150°C is shown in Fig. 1 where conversion is plotted against catalyst weight/flow rate (W/F) for two different weights of catalyst. The fact that the data from the two

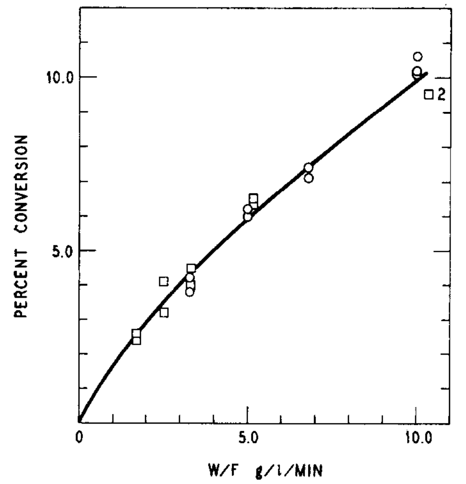

FIG. 1. Conversion vs W/F for the cobalt molybdate-alumina catalyst at 150°C: ○, 0.600 g of catalyst sample; □, 0.300 g of catalyst sample.

catalyst weights fall on the same conversion curve is indicative of no interphase diffusional effects. Two particle sizes (20–35 and 35–60 mesh) were compared and found to have the same activity per gram.

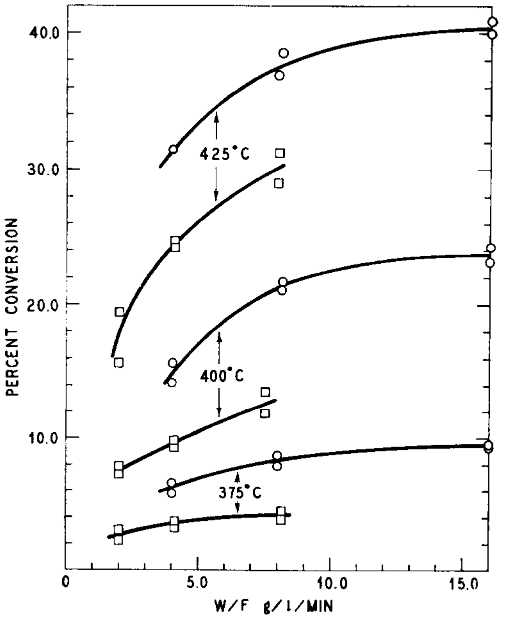

FIG. 2. Conversion vs W/F for the WO_3-silica catalyst at 375, 400, and 425°C in a quartz reactor (0.66 cm^2 cross section): ○, 0.800 g of catalyst sample; □, 0.400 g of catalyst sample.

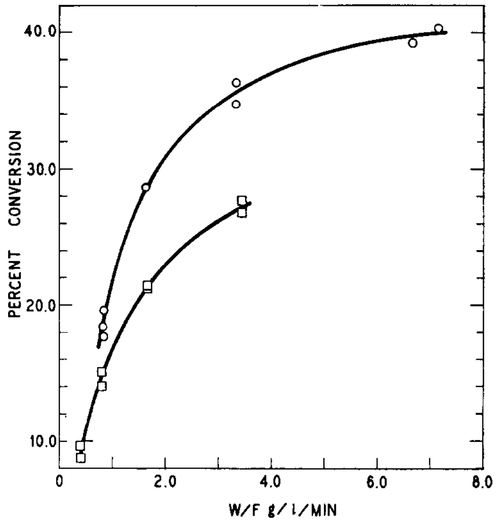

FIG. 3. Conversion vs W/F for the WO_3-silica catalyst at 460°C in a quartz reactor (0.10 cm^2 cross section), ○, 0.200 g of catalyst sample, □, 0.100 g of catalyst sample.

Hence it was concluded that propylene disproportionation on cobalt molybdate–alumina is not limited by interphase or pore diffusional effects.

When similar studies were made using the 6.8% WO_3-silica catalyst at 375, 400, and 425°C, the results shown in Fig. 2 were obtained which are indicative of interphase mass transfer limitations. In a smaller reactor at 450°C at weight hourly space velocities (WHSV) as high as 200 g/g/hr, as shown in Fig. 3, a mass transfer problem is still evident. A comparison of two different particle sizes (20–35 and 35–60 mesh) for this 6.8% WO_3 on silica catalyst showed approximately equal activity per gram. However, catalyst preparation in this case did not produce a uniform distribution of the WO_3 promoter on the entire catalyst surface; hence an unusual activity vs particle size relationship is not surprising.

A silica support impregnated with approximately 0.1% WO_3 was found to have the typical conversion vs W/F characteristics of interphase mass transfer limitations at 460°C. A comparison of 20–35 mesh vs 35–60 mesh particles showed the smaller particles to have approximately

2X the activity per gram of the larger particles, which is also characteristic of a diffusion limited reaction.

By the classical methods of Hougen and Watson (*2*), a material balance in a section of the catalyst bed under steady state conditions equates the rate of disappearance of reacting gas to the rate of mass transfer across the interface per unit time. For an equilibrium reaction the integrated form of the equation is:

$$\ln\left(\frac{Y_{\mathrm{in}} - Y_{\mathrm{eq}}}{Y_{\mathrm{out}} - Y_{\mathrm{eq}}}\right) = \frac{k_G P a m}{G_M A_d} = \frac{0.357am}{\epsilon A_d (N_{\mathrm{Sc}})^{2/3} (N_{\mathrm{Re}})^{0.359}}, \quad (1)$$

where the Reynolds (N_{Re}) and Schmidt (N_{Sc}) number correlation of Petrovic and Thodos (*3, 4*) for low Reynolds numbers is used; Y refers to mole fraction of propylene in, out, and at equilibrium (~ 0.55); a, m, ϵ, and A_d are, respectively, the external surface area (~ 250 cm^2/g), weight of catalyst in grams (0.800), void fraction (0.40), and reactor cross-sectional area (0.66 cm^2). Using the data from Fig. 2 (400°C, 0.800 g of catalyst, $W/F = 4.0$) and calculated N_{Sc} and N_{Re} of 0.755 and 3.25, respectively, the rhs of Eq. (1) equals 213 while experimentally the lhs of Eq. (1) equals 0.345. Hence, the rate of mass transfer to the total external, catalyst surface is approximately three orders of magnitude larger than the observed reaction rate.

Since the propylene mass transfer rates to catalyst particles should be comparable or perhaps even greater for the WO_3–silica catalyst at the higher temperature, it seems incongruous that the cobalt molybdate–alumina catalyst has no diffusion limitation while the WO_3–silica catalyst (even at lower levels of activity per gram) is markedly limited by mass transfer effects. Perhaps one is comparing the activity of a large number of moderately active sites on the entire cobalt molybdate catalyst surface with the activity of a much smaller number of very active sites on the external surface of the tungsten catalyst. Even though propylene may be transferred to the total, external, catalyst surface 100 to 10000 times faster than product is formed, widely separated and very active sites could have their inherent activities limited by localized film diffusional effects which are also a function of Reynolds and Schmidt numbers. For example, a catalyst having 6.8% WO_3 on silica with 345 m^2/g of surface area would have only 5% or 17.3 m^2/g of the total surface covered by the WO_3 promoter. Thus, an effective diffusional surface area for 0.059-cm diameter particles, when all the WO_3 participates in the reaction, would be 12.5 cm^2/g or 5% of the external surface area of 250 cm^2/g. Since only a small percentage of the promoter would be expected to be active, the effective external surface area would be an even smaller percentage of the total external, particle surface area.

Where only a small fraction of the available sites are active, the classical prediction (*5*) of a very low temperature dependency for interphase diffusional effects is probably not accurate. If the surface is heterogeneous, an increase in temperature could activate sites that are inactive at lower temperatures. The net result is an increase in the total number of sites (and active site area) for the diffusion limited process and a temperature dependence which perhaps can be approximated by an Arrhenius type equation. The data plotted in Fig. 2 shows a temperature dependency (30–45 kcal) which is greater than that expected from classical considerations where the activation energy should be near zero (*5*).

It is concluded that perhaps the only accurate way to determine the importance of interphase diffusional effects on observed reaction rates is to follow conversion changes as a function of particle Reynolds number. Calculations made on the basis of generalized equations for diffusion which use total external, particle surface area instead of an effective site area can be very misleading. Also high apparent activation energies could exist for reactions which are limited by mass transfer to catalyst particles in spite of classical considerations which suggest values near zero.

REFERENCES

1. Begley, J. W., and Wilson, R. T., *J. Catal.* **9**, 375 (1967).
2. Hougen, O. A., and Watson, K. M., "Chemical Process Principles," Chap. 20. Wiley, New York, 1947.
3. Petrovic, L. J., and Thodos, G., *Ind. Eng. Chem. Fundam.* **7**, 274 (1968).
4. Satterfield, C. N., "Mass Transfer in Heterogeneous Catalysis," Chap. 2, M.I.T. Press, Cambridge, Mass., 1970.
5. Carberry, J. J., *Catal. Rev.* 3(1), 61 (1969).

A. J. Moffat
M. M. Johnson
Alfred Clark

Phillips Petroleum Company,
Bartlesville, Oklahoma 74003

Received December 19, 1969

Thermal Decomposition of Ammonium Y Zeolite

Products formed by the thermal decomposition of ammonium Y zeolite have recently been discussed (*1–4*). By calcining at 500°C in shallow and deep beds, or by using calcination conditions such that the decomposition product gases remain in the vicinity of the zeolite, different products were obtained. The products have been distinguished by their hydrothermal stabilities, thermograms, reactivity to ammonia, ion-exchange and adsorptive capacities, silica to alumina ratios, and by differential thermal analysis (*1–4*).

Kerr (*2*) has suggested a mechanism for the stabilization process in which tetrahedrally coordinated aluminum ions are split out of the zeolite lattice and new Si–O–Si bonds are formed. It was concluded from thermogravimetric studies that the final form of the zeolite after calcination for 2–4 hr at 700–800°C contained no chemical water. The suggested mechanism is:

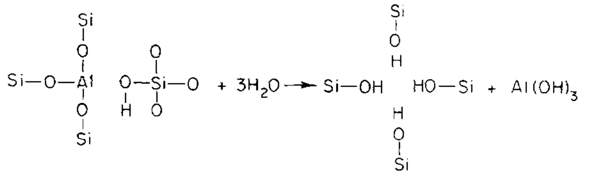

$$\mathrm{Si{-}O{-}\underset{\underset{Si}{|}}{\underset{O}{|}}{\overset{\overset{Si}{|}}{\overset{O}{|}}{Al}}\quad \underset{H}{O}{-}\underset{O}{\overset{\overset{O}{|}}{Si}}{-}O + 3H_2O \longrightarrow Si{-}OH\quad \underset{\underset{\underset{Si}{|}}{O}}{H}\ \overset{\overset{\overset{Si}{|}}{O}}{H}\quad HO{-}Si + Al(OH)_3} \qquad (1)$$

The four SiOH groups were believed to condense to form Si–O–Si bonds and water.

However, Kerr (*1*) has reported that after calcination at 500°C, the stabilized zeolite still contains about half as much chemical water as hydrogen Y zeolite. This chemical water could be present in the form of –SiOH or –AlOH groups.

In order to study the structural surface groups on Y zeolites, the decomposition of ammonium Y zeolite has been studied using thermal analysis, infrared spectroscopy, ion-exchange and X-ray diffraction. For comparison with the ultrastable zeolite, an ammonium Y zeolite stabilized by multivalent cations (magnesium) was studied. The zeolite composition has previously been shown to be hydrothermally stable up to high temperatures in contrast to ammonium and sodium ammonium Y zeolites.

Ammonium Y was prepared and decomposed by Procedure A of McDaniel and Maher (*3*) except that the second calcina-

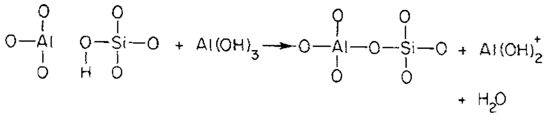

$$\mathrm{O{-}\underset{O}{\overset{\overset{O}{|}}{Al}}\quad \underset{H}{O}{-}\underset{O}{\overset{\overset{O}{|}}{Si}}{-}O + Al(OH)_3 \longrightarrow O{-}\underset{O}{\overset{\overset{O}{|}}{Al}}{-}O{-}\underset{O}{\overset{\overset{O}{|}}{Si}}{-}O + Al(OH)_2^+ + H_2O} \qquad (2)$$